Liquid Crystals
Publication details, including instructions for authors and subscription information:
http://www.informaworld.com/smpp/title~content=t713926090

Light scattering measurements of anisotropic viscoelastic coefficients of a main-chain polymer nematic liquid crystal

Sin-Doo Lee[a]; R. B. Meyer[a]
[a] Department of Physics, Brandeis University, Waltham, Massachusetts, U. S. A.

To cite this Article Lee, Sin-Doo and Meyer, R. B.(1990) 'Light scattering measurements of anisotropic viscoelastic coefficients of a main-chain polymer nematic liquid crystal', Liquid Crystals, 7: 1, 15 — 29
To link to this Article: DOI: 10.1080/02678299008029190
URL: http://dx.doi.org/10.1080/02678299008029190

LIQUID CRYSTALS, 1990, VOL. 7, NO. 1, 15–29

Light scattering measurements of anisotropic viscoelastic coefficients of a main-chain polymer nematic liquid crystal

by SIN-DOO LEE† and R. B. MEYER
Department of Physics, Brandeis University, Waltham, Massachusetts 02254, U.S.A.

We report the first systematic measurements of elastic coefficients and viscosities that clearly demonstrate the distinction between rigid and semiflexible behaviour of a main-chain polymer nematic liquid crystal, a solution of poly-γ-benzyl glutamate (PBG) in mixed organic solvents. Quasi-elastic Rayleigh scattering studies show a crossover which occurs at a molecular chain length near the persistence length of PBG as the chain length increases. The results are in qualitatively good agreement with recent theoretical predictions for semiflexible chains. It is seen that bending distortions of an individual polymer play an important role in the fundamental nature of nematic elasticity and viscosity.

1. Introduction

Concentrated solutions of long polymers may exhibit one or more liquid-crystalline phases between a conventional liquid and a crystalline solid. Study of these polymer liquid crystals provides us with fundamental knowledge about the intrinsic properties of polymers and low-molecular-weight liquid crystals. Also, the high degree of anisotropy in the elasticity and viscosity of their liquid crystals is of great significance for both the discovery of new macroscopic structural phenomena [1, 2] and the industrial application [3] of these materials.

Measurements of the basic mechanical properties of these systems should be useful both as a basis for understanding their phenomenology and as a guide to the development of theory relating their molecular and macroscopic properties. It is of fundamental importance to understand completely their anisotropic mechanical properties reflecting structural features in terms of their intrinsic molecular parameters such as the length-to-diameter ratio, L/d, the degree of chain flexibility, and the volume fraction, ϕ, of the polymer in solution.

There are several ways [4] of measuring the viscous and elastic coefficients of liquid crystals. Among them, quasi-elastic depolarized Rayleigh scattering has been a very effective method, particularly for polymer nematic liquid crystals formed from solutions of long rigid or semirigid macromolecules such as PBG, because the high anisotropy in their viscoelasticity produces unusual static and dynamic responses to the external electric and magnetic fields [1]. Studies of both the mean intensity of the scattered light and its time dependence, due to thermal fluctuations of the nematic director field, enable us to determine ratios of elastic moduli to one another, and ratios of elastic moduli to effective viscosities associated with the elastic distortion modes.

We present in this paper the complete study of the crossover from rigid to semiflexible behavior of elastic coefficients and viscosities of a main-chain polymer

† Present address: Bellcore, 331 Newman Springs Road, Red Bank, New Jersey 07701, U.S.A.

0267–8292/90 $3.00

nematic liquid crystal, formed from a solution of poly-γ-benzyl-glutamate (PBG) in mixed organic solvents, as the importance of molecular chain flexibility increases with chain length. Preliminary description of the crossover behavior has been reported previously [5]. We performed quasi-elastic depolarized Rayleigh scattering on well oriented planar samples. In §2 we describe the PBG nematic systems we studied and the surface treatment for achieving planar alignment of PBG. In §3 quasi-elastic light scattering due to the orientational fluctuations and the two scattering geometries we used are described in detail. The experimental results for anisotropic viscous and elastic coefficients of PBG nematics are presented in §4. We also compare them with existing theoretical predictions to test several theories qualitatively. In the remaining section we discuss the main features of the experimental results, and draw some conclusions.

2. PBG nematic systems

The most extensively studied class of polymer liquid crystals is that of the synthetic polypeptides which exhibit liquid crystalline phases in their rod-like helical conformations. Due to its ready availability and good solubility characteristics, PBG has been extensively studied, and it is currently the best characterized polymer liquid crystal [2, 5–9]. A complete picture of the viscous and elastic behavior of PBG nematic systems, however, has not so far been given in a systematic way.

Above a certain volume fraction of the polymer, PBG froms a lyotropic liquid crystal in a number of organic solvents and mixed solvent systems, including benzene, nitrobenzene, chloroform, pyridine, *N*,*N*-dimethylformamide (DMF), dichloroacetic acid (DCA), *m*-cresol, dioxane, and dichloromethane (CH_2Cl_2). It has been shown that in all circumstances in which PBG forms the liquid-crystalline phase it is in the extended α-helical molecular conformation. The persistence length of PBG in several solvents has been found [10–12] to be in the range 750 Å to 1,200 Å, indicating that the polymer may possess limited flexibility.

The α-helical conformation itself has the following characteristics [13]: The backbone chain of the polypeptide repeats exactly 3·6 amino acid residues per five turns of the helix. Each successive residue translates 1·5 Å along the helix axis, and the residue molecular is 219. The internal degrees of freedom in the side-chain yield a variety of side-chain secondary structures and lead to considerable variation in the diameter of PBG in solution. The diameter of α-helical PBG is about 15 Å to 25 Å, determined by X-ray measurements [10].

We studied nematic solutions of PBG of several molecular weights in the range 6·6 to 21·0 $\times$ 10^4 (from Sigma Chemical Co. and U.S. Biochemical Corp.), giving L/d = 32 to 100. Freeze-dried PBG with 50–50 weight ratios of PBLG and PBDG (M_w = 15·0 $\times$ 10^4) was also prepared. The average molecular weight of the 50–50 mixture is estimated as $\bar{M}_w = xM_w(\mathrm{LG}) + (1 - x)M_w(\mathrm{DG})$, where x denotes the molar fraction of PBLG. We used a solvent mixture composed of 18 per cent dioxane and 82 per cent dichloromethane to suppress the cholesteric helicity, and added to this a few per cent of DMF to prevent the polymer from aggregating [14]. No evidence of aggregation was seen. The solvent compensation of the helicity may not be expected to yield the perfect nematic phase since other factors such as temperature and the concentration also play a role in determining the sense and pitch of the cholesteric helix. The pitch of the helix decreases as the concentration increases. In practice, what can be achieved is to make the sample thickness be on order of the pitch of the

resulting cholesteric helix, and thus suppress static twisting in samples with rigid boundary alignment.

Each PBG solution was made up by dissolving the weighed PBG in the weighed solvent mixture in a 1·0 ml centrifuge vial. For conversion to the volume fraction, we took the specific volume of PBG as 0·791 ml/g [15] and the density of the mixed solvent as 1·28 g/ml. We neglected any contraction of PBG on dissolving and determine the volume fraction, ϕ, of each PBG solution. The average molecular weights, the average length-to-diameter ratios, and the volume fractions of PBG nematic systems we studied are summarized in table 1.

Table 1. The average molecular weights, the average length-to-diameter ratios, and the volume fractions of the PBG systems we studied. L and R denote PBLG and racemic PBG (50–50 weight ratio of PBLG and PBDG), respectively.

Sample number	Molecular weight ($\bar{M}_w \times 10^{-4}$)	Degree of polymerization D.P.	Length-to-diameter ratio L/d	Volume fraction ϕ
1	7·0 (L)	320	32	0·159
2	7·0 (L)	320	32	0·203
3	8·5 (L)	390	39	0·158
4	8·5 (L)	390	39	0·196
5	6·6/15·0 (R)	420	42	0·157
6	8·5/15·0 (R)	500	50	0·155
7	11·0/15·0 (R)	580	58	0·156
8	11·0/15·0 (R)	580	58	0·202
9	16·5/15·0 (R)	720	72	0·154
10	16·5 (L)	750	75	0·152
11	19·0 (L)	870	87	0·158
12	21·0 (L)	1,000	100	0·154

For a polymer liquid crystal of very long molecules, it has been argued [16] that the nematic director must lie parallel to a surface, because condensation of many chain ends at the surface costs a greal deal of entropy. Therefore, the homeotropic alignment will not be favoured unless there is a strong binding energy for chain ends at the surface. The development of homeotropy at the surface will thus depend both on molecular chain length and on the detailed chemistry of the surface.

For PBG, however, the previous experiments suggest that all of the standard procedures for producing parallel surface alignment, that proved successful in low-molecular-weight liquid crystals, have yielded only the homeotropic alignment [17, 18]. This is probably due to some binding of the polymer ends to glass. Following the technique developed by Taratuta *et al.* [19], we achieved the planar alignment of PBG, parallel to the glass surface coated with an inert plasma-polymerized ethylene film, by placing the sample, just after filling, in about a 20 kG magnetic field. Although initial uniformity of the alignment produced by the magnetic field was somewhat diminished after the sample was taken out of the field, a strong memory effect remained in the direction of the aligning field. The strength of the uniform anchoring was enhanced by applying a thin layer of SiO_x, evaporated obliquely onto the glass surface prior to coating with polyethylene. The detailed experimental procedure and the optimum conditions regarding the surface alignment of PBG on a plasma-polymerized ethylene film are described elsewhere [19]. We used PBG sample cells, typically 50 μm thick, with planar as well as homeotropic boundary conditions to

carry out both the external field effect and light scattering experiments on the same cell.

3. Quasi-elastic light scattering

Long ago, the Orsay Liquid Crystal Group [20, 21] predicted theoretically and confirmed experimentally that long-wavelength fluctuations of the nematic director **n** give rise to two overdamped periodic distortion modes, associated with splay-bend ($\alpha = 1$) and twist-bend ($\alpha = 2$) elastic distortions of nematic liquid crystals. The local orientational fluctuations $\delta\mathbf{n}(\mathbf{r}, t) = \mathbf{n}(\mathbf{r}, t) - \mathbf{n}_0$ of the nematic director around its equilibrium value $\mathbf{n}_0$ can be written as a sum of the two normal modes. These orientational fluctuations cause strong depolarized scattering of the light. In the absence of external fields, the differential cross section per unit scattering volume per solid angle $d\Omega$ is given by the following equation in terms of the mean-square amplitude of the fluctuations in each mode:

$$\frac{d\sigma}{d\Omega} = \pi^2\lambda^{-4}\varepsilon_a^2 \sum_\alpha G_\alpha^2 \langle|\delta n_\alpha(\mathbf{q})|^2\rangle \quad (\alpha = 1, 2), \tag{1}$$

where ε_a denotes the dielectric anisotropy ($\varepsilon_\parallel - \varepsilon_\perp$), λ the wavelength of the light, G_α a geometric factor involving the polarization vectors of the incoming ($\hat{i}$) and the scattered ($\hat{f}$) light. The scattering wavevector **q** (i.e., the difference between the wavevectors of the incoming and the scattered light) has two components, $q_\parallel$ and $q_\perp$, parallel and normal to the director $\mathbf{n}_0$, respectively.

From the equipartition theorem, i.e., the energy in each mode is $1/2kT$, the basic equation for the Fourier decomposed fluctuation (per unit volume) can be written as

$$\langle|\delta n_\alpha(\mathbf{q})|^2\rangle = \frac{kT}{K_\alpha(\mathbf{q})} \quad (\alpha = 1, 2), \tag{2}$$

with $K_\alpha(\mathbf{q}) = K_3 q_\parallel^2 + K_\alpha q_\perp^2$. The factor G_α is given by $(f_\alpha i_3 + f_3 i_\alpha)$ in an orthonormal coordinate system of which the basis vectors are $\mathbf{e}_3 = \mathbf{n}_0$, $\mathbf{e}_2 = (\mathbf{n}_0 \times \mathbf{q})/|\mathbf{n}_0 \times \mathbf{q}|$, and $\mathbf{e}_1 = \mathbf{e}_2 \times \mathbf{n}_0$.

Since the two uncoupled fluctuation modes are both overdamped, their time dependence obeys a diffusion-type differential equation described by hydrodynamic equations. Experimentally, these time dependent fluctuations lead to a frequency modulation of the scattered light, and can be observed with current optical techniques. The resulting relaxation equation for each mode has the form

$$\eta_\alpha(\mathbf{q}) \frac{\partial}{\partial t} n_\alpha(\mathbf{q}) = K_\alpha(\mathbf{q})\nabla^2 n_\alpha(\mathbf{q}), \quad (\alpha = 1, 2), \tag{3}$$

with the relaxation time constant $\tau_\alpha = \eta_\alpha(\mathbf{q})/K_\alpha(\mathbf{q})$. Here $\eta_\alpha(\mathbf{q})$ is the effective viscosity which is a function of five independent viscosity coefficients [22] and the scattering wavevector **q**. Two configurations are of special interest. If **q** is along the director, the deformation for both modes reduces to a pure bend, and $\eta_{1,2}(\mathbf{q}) \equiv \eta_{\text{bend}} = \gamma_1 - \alpha_2^2/\eta_c$. If **q** is normal to the director, mode 2 becomes a pure twist deformation, of viscosity $\eta_2(\mathbf{q}) \equiv \eta_{\text{twist}} = \gamma_1$. Mode 1 is then a case of pure splay, and $\eta_1(\mathbf{q}) \equiv \eta_{\text{splay}} = \gamma_1 - \alpha_3^2/\eta_b$.

The light source was the 5,145 Å line of an argon ion laser at a power of about 100 mW. No evidence of sample heating was present during the experiment. The signal was detected with a photo-multiplier; the photoelectron pulses were

standardized and sent to a digital correlator which computes the temporal autocorrelation function of the intensity fluctuations of the scattered light in real time. We studied two scattering geometries (for details, see [9]) in samples with parallel boundary conditions. In the first the nematic director **n** is perpendicular to the scattering plane, with the incident polarization $\hat{i}$ parallel to the director **n**, and the scattered polarization $\hat{f}$ parallel to the scattering plane. The plane of the sample is oriented so that the scattering wavevector **q** is parallel to the glass windows ($q_{\parallel} = 0$). In the second geometry, everything is the same as in the first, except that the sample is rotated with respect to an axis normal to its surface so that the director **n** is parallel to the scattering wavevector **q** ($q_{\perp} = 0$).

The first geometry allows us to see scattering from a superposition of pure splay and pure twist distortions. The ratio of the amplitudes of these distortions depends on the ratio of twist and splay elastic moduli, and their relaxation times depend on their effective diffusivities. The relative amplitudes are proportional to $\cos^2(\theta/2)/K_1q^2$ for splay and $\sin^2(\theta/2)/K_2q^2$ for twist, where θ is the total scattering angle. In the

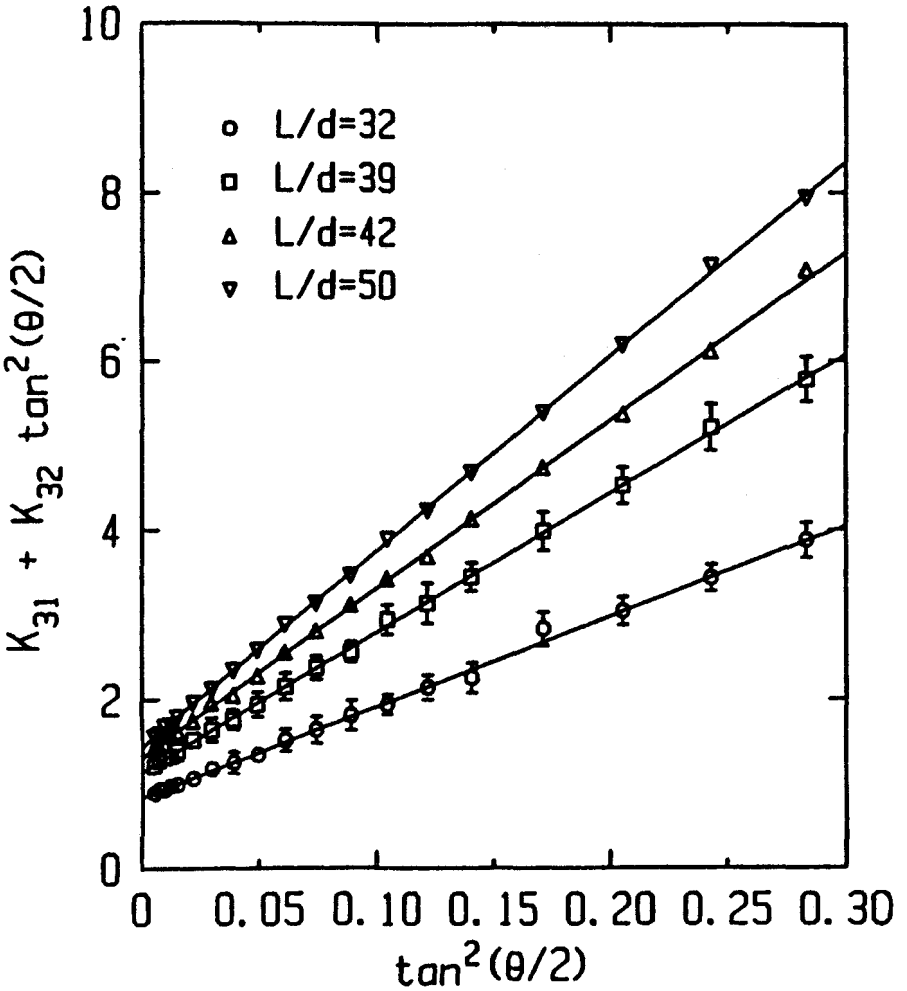

Figure 1. Ratios of total scattering amplitudes of the elastic distortion modes in the two geometries in the PBG nematic systems having $L/d = 32$–50 at $\phi \approx 0{\cdot}16$. K_{31} and K_{32} denote K_3/K_1 and K_3/K_2, respectively.

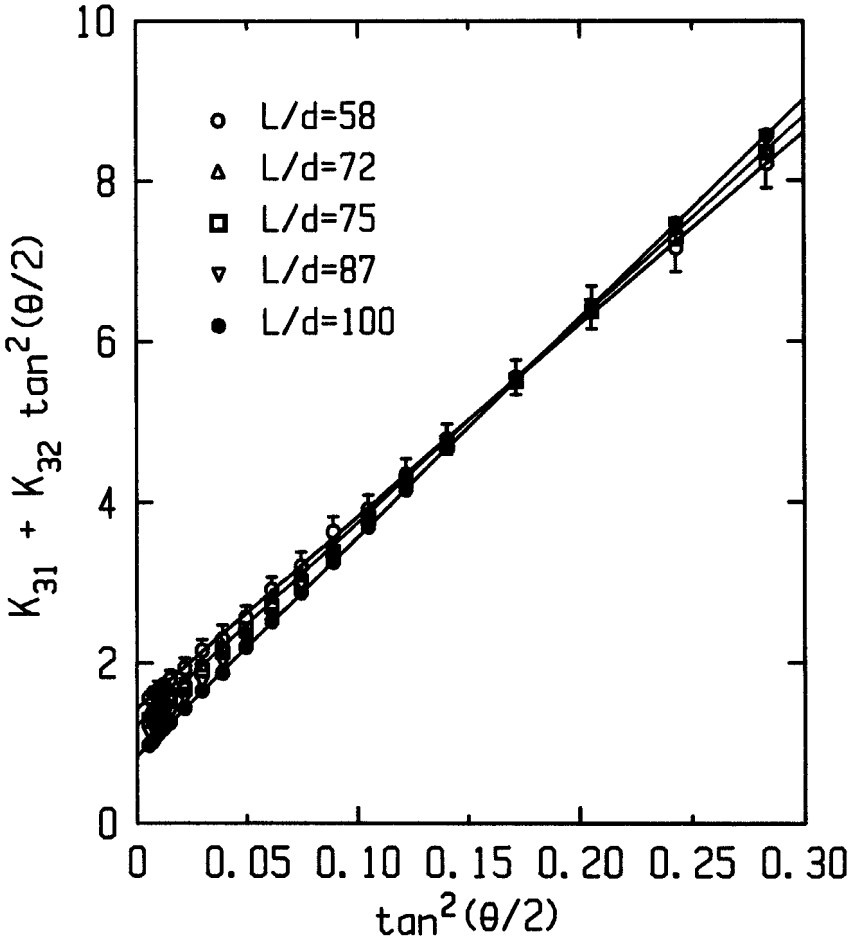

Figure 2. Ratios of total scattering amplitudes of the elastic distortion modes in the two geometries in the PBG nematic systems having L/d = 58–100 at $\phi \approx 0{\cdot}16$. K_{31} and K_{32} denote K_3/K_1 and K_3/K_2, respectively.

second geometry we see scattering from a pure bend distortion. The amplitude for pure bend is proportional to $\cos^2(\theta/2)/K_3q^2$. Also, the relaxation time of the bend distortion determines another effective diffusivity. Keeping the entire scattering geometry fixed and switching from the first sample orientation to the second, we can compare the amplitudes of the pure bend distortion to the splay and twist distortions as follows:

$$\frac{a_1 + a_2}{a_3} = \frac{K_3}{K_1} + \frac{K_3}{K_2}\tan^2\frac{\theta}{2}, \tag{4}$$

where a_1, a_2 and a_3 are the amplitudes of splay, twist and bend signals, respectively. The measurements were performed at a number of scattering angles to confirm the correct angular dependence of the scattering intensities and relaxation times, and repeated at least 10 times at each scattering angle.

A functional dependence of the relationship equation (4) is illustrated for a variety of L/d in figures 1 and figure 2 as a function of $\tan^2(\theta/2)$. The least-square straight lines,

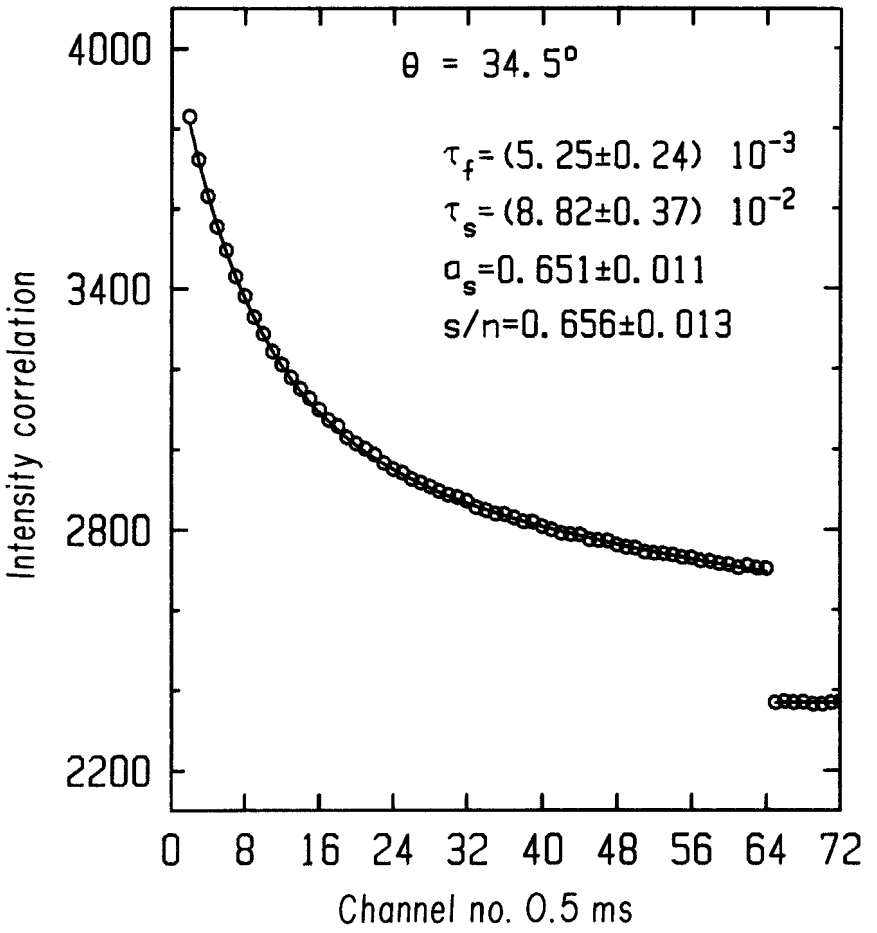

Figure 3. A typical intensity autocorrelation function composed of the splay and twist distortions, fitted to a combination of two exponentials, in a PBG nematic system. (L/d = 39 and $\phi \approx 0{\cdot}20$).

weighted inversely by the standard deviation of the data at each scattering angle, fit reasonably well the experimental data. K_3/K_1 and K_3/K_2 are then directly measured from the intercept and the slope, respectively, as shown in figures 1 and 2. In addition, the value of K_1/K_2 determined from the nonlinear least-squares fitting of the splay-twist intensity autocorrelation function over a wide range of scattering angles is consistent with the value given by the intensity measurements. A typical intensity autocorrelation function composed of splay and twist distortions is shown in figure 3, fitted to a combination of two exponentials with four parameters: signal-to-noise ratio (s/n), the amplitude of slow mode (a_s), and two distinct relaxation times (τ_s and τ_f). This was relatively easy because the two relaxation times were well separated.

4. Anisotropic viscous and elastic coefficients

Analysis of the intensity of the scattered light and the relaxation times of the characteristic director fluctuations produces all the ratios of elastic moduli to one

Table 2. Ratios of the elastic moduli K_3/K_1 and K_3/K_2 determined from intensity measurements, and K_1/K_2 from the intensity autocorrelation function composed of the splay and twist modes, fitted to a combination of two exponentials, in the PBG nematic systems.

Sample	K_3/K_1	K_3/K_2	K_1/K_2
1	0·84 ± 0·05	10·7 ± 0·6	12·5 ± 1·1
2	1·05 ± 0·07	17·8 ± 1·1	17·1 ± 1·4
3	1·14 ± 0·08	16·5 ± 0·9	14·5 ± 1·1
4	1·38 ± 0·12	24·7 ± 1·5	18·4 ± 1·4
5	1·32 ± 0·09	19·9 ± 1·1	14·8 ± 1·1
6	1·44 ± 0·11	23·1 ± 1·3	16·1 ± 1·1
7	1·43 ± 0·12	24·0 ± 1·4	17·2 ± 1·5
8	1·41 ± 0·12	29·3 ± 1·9	22·2 ± 1·5
9	1·21 ± 0·10	25·3 ± 1·6	22·4 ± 1·5
10	1·14 ± 0·08	25·4 ± 1·6	23·2 ± 1·4
11	0·97 ± 0·05	26·7 ± 1·6	26·6 ± 1·5
12	0·83 ± 0·04	27·3 ± 1·7	31·2 ± 1·7

Table 3. The orientational diffusivities, determined from the intensity autocorrelation functions, and the resulting ratios of effective viscosities in the PBG nematic systems.

Sample	η_{splay}/K_1 $\times 10^7$ s/cm^2	γ_1/K_2 $\times 10^8$ s/cm^2	η_{bend}/K_3 $\times 10^5$ s/cm^2	η_{splay}/γ_1	γ_1/η_{bend}	η_c/η_b
1	3·11 ± 0·16	4·56 ± 0·19	3·96 ± 0·18	0·85 ± 0·04	108 ± 9	92 ± 9
2	4·06 ± 0·16	7·52 ± 0·32	2·54 ± 0·12	0·92 ± 0·05	166 ± 14	153 ± 15
3	3·88 ± 0·15	6·43 ± 0·25	2·87 ± 0·15	0·88 ± 0·04	136 ± 12	120 ± 12
4	5·99 ± 0·22	11·8 ± 0·9	2·31 ± 0·12	0·93 ± 0·04	207 ± 22	193 ± 21
5	5·04 ± 0·18	8·14 ± 0·27	2·93 ± 0·14	0·92 ± 0·05	140 ± 11	129 ± 12
6	6·80 ± 0·29	11·7 ± 0·9	2·98 ± 0·13	0·94 ± 0·05	170 ± 17	160 ± 18
7	8·09 ± 0·42	14·3 ± 1·0	4·02 ± 0·21	0·97 ± 0·04	148 ± 15	144 ± 16
8	10·4 ± 0·7	23·1 ± 1·2	3·11 ± 0·16	1·00 ± 0·06	254 ± 24	254 ± 28
9	10·5 ± 0·9	23·5 ± 1·1	5·07 ± 0·26	0·99 ± 0·05	187 ± 17	185 ± 19
10	12·4 ± 1·0	28·8 ± 1·7	5·58 ± 0·28	1·00 ± 0·04	203 ± 20	203 ± 21
11	14·0 ± 1·0	37·1 ± 2·1	5·48 ± 0·30	1·00 ± 0·06	254 ± 24	254 ± 27
12	14·6 ± 1·1	45·7 ± 2·4	5·39 ± 0·26	1·00 ± 0·05	311 ± 29	311 ± 32

another and the orientational diffusivities. Our experimental results for ratios of the elastic moduli are collected in table 2.

The inverse orientational diffusivities, determined from the intensity autocorrelations, and the resulting ratios of effective viscosities, are presented in table 3 as a function of L/d. We checked that the relaxation rates are proportional to q^2, confirming the diffusive character of the elastic distortion modes. The diffusivities exhibit large anisotropies, which makes the separation of the twist and splay modes relatively easy.

4.1. *Elastic moduli*

First we discuss the elastic moduli. The measured K_1 and K_3 are of the same order of magnitude, about ten times larger than K_2. But, the most striking result is the behavior of K_3/K_1, as shown in figure 4, which initially increases with L/d, reaches a maximum and then decreases. To interpret this behaviour, we look at K_1 and K_3 separately. Recent experimental work [23, 24] on PBG has shown that K_2 remains essentially constant in the molecular weight range of 9·6 to 24·6 $\times 10^4$, and exhibits no dependence on the concentration. Thus, K_2 might be expected to remain rather

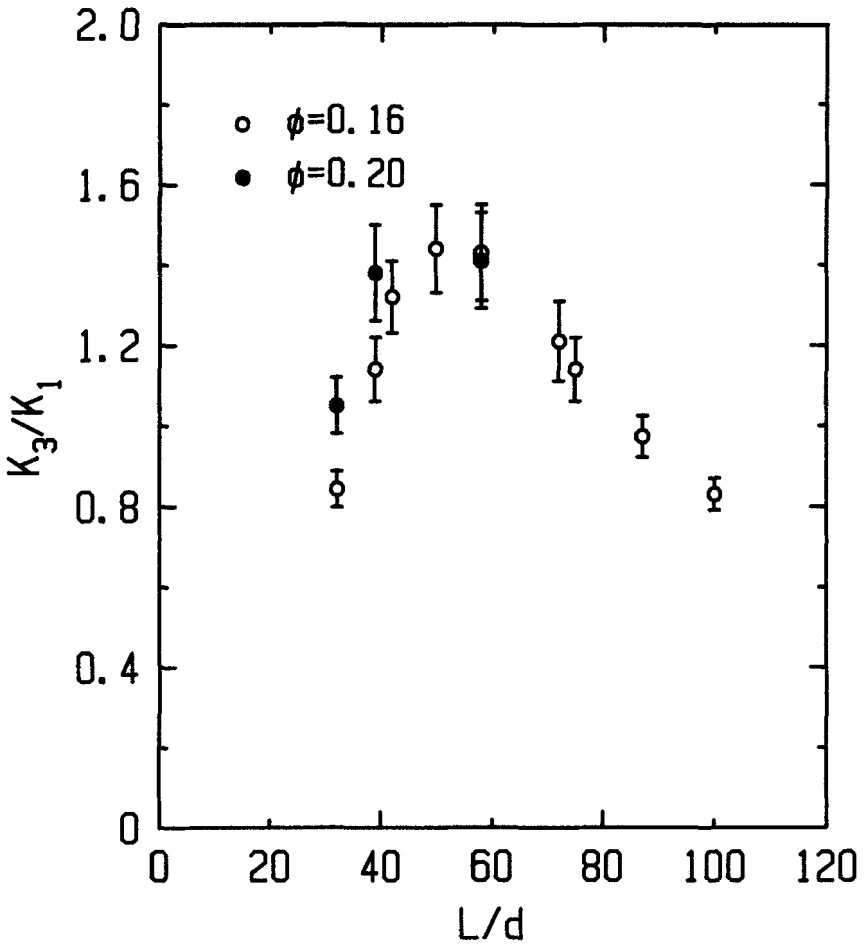

Figure 4. Ratio of the elastic moduli K_3/K_1 as a function of L/d in the PBG nematic systems.

constant in the range of values we studied. Assuming K_2 constant, with a literature value [6, 24] of $K_2 = 0{\cdot}6 \times 10^{-7}$ dynes, we determined the absolute magnitudes of K_1 and K_3 which were plotted in figures 5 and 6 as a function of L/d. K_1 exhibits nearly linear dependence on L/d over the entire range studied. For K_3, a crossover from a rapidly increasing dependence to a saturation with increasing L/d is observed. The crossover begins at $L/d \approx 50$.

We now compare the behavior of the measured elastic moduli of PBG with existing theoretical predictions. Simple models of the elastic moduli of nematic liquid crystals composed of long polymer chains treated the molecules as interacting only through hard-core repulsions. For rigid rods, this implies that the elastic free energy arises only from entropic effects. In the limit of highly ordered rigid rods, the two body excluded volume interactions lead to [25, 26]

$$\left.\begin{aligned} K_1 &\approx \frac{kT}{d}\frac{7}{8\pi}\phi\left(\frac{L}{d}\right) = 3K_2, \\ K_3 &\approx \frac{kT}{d}\frac{4}{3\pi^2}\phi^3\left(\frac{L}{d}\right)^3. \end{aligned}\right\} \tag{5}$$

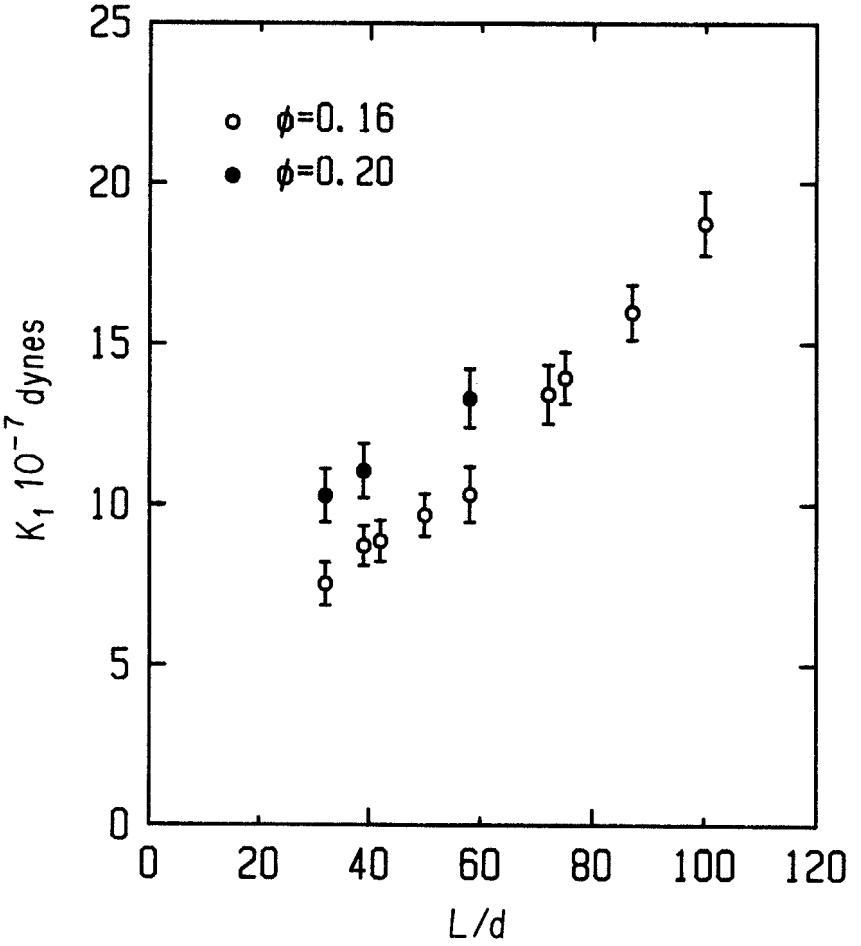

Figure 5. Estimated values for K_1 as a function of L/d, assuming $K_2 = 0{\cdot}6 \times 10^{-7}$ dynes, in the PBG nematic systems.

The bend modulus K_3 is by far the largest, and the splay K_1 is three times the twist modulus K_2. In contrast, for polymers which are semiflexible, but still fully extended parallel to the nematic director, bending of the polymers to follow the director distortions implies storage of bending elastic energy in the polymer chains; K_3 becomes independent of chain length and linear in ϕ. More quantitatively, the scaling nature [27] of a semiflexible chain leads to

$$\left.\begin{aligned} K_2 &\approx \frac{kT}{d}\,\phi^{1/3}\left(\frac{P}{d}\right)^{1/3}, \\ K_3 &\approx \frac{kT}{d}\,\phi\left(\frac{P}{d}\right). \end{aligned}\right\} \tag{6}$$

where P is the persistence length of the chain.

Moreover, Meyer [16] argued that for both rigid and semiflexible polymers, the splay free energy is dominated by the entropy of the chain ends, whose concentration is changed by splay distortion, so that K_1 is linear in both L/d and ϕ, and becomes larger than K_3 for long chains. It should be noted that de Gennes proposed a model for the splay modulus for semiflexible molecules, [28], based on intermolecular strain

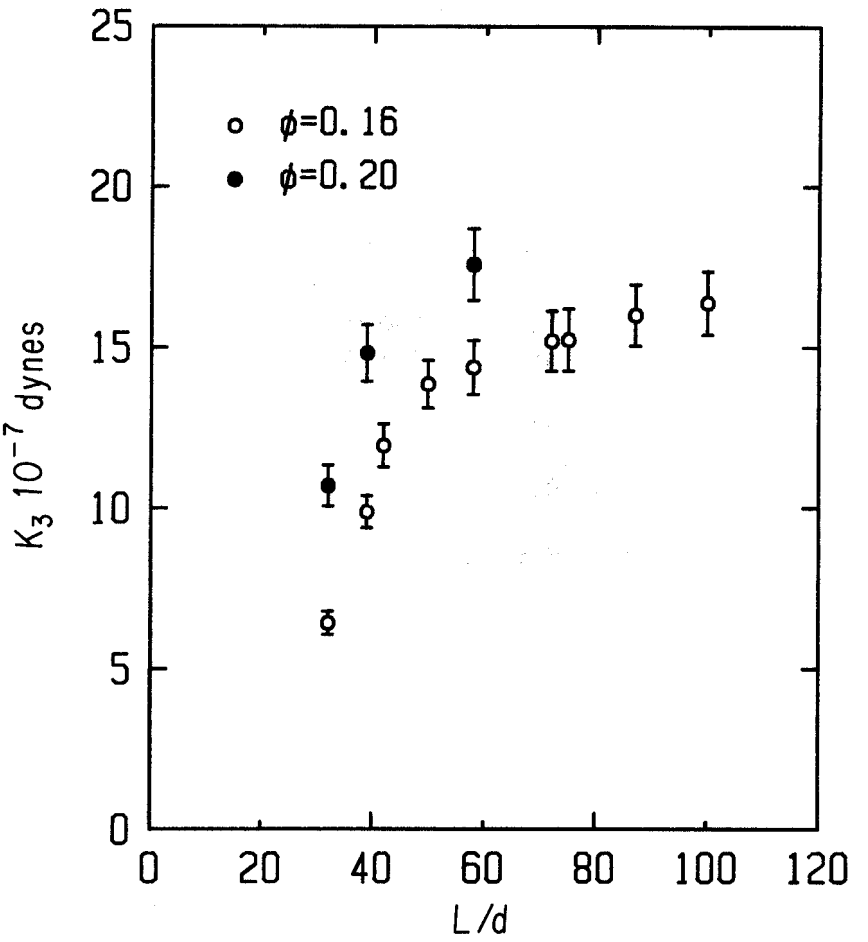

Figure 6. Estimated values for K_3 as a function of L/d, assuming $K_2 = 0{\cdot}6 \times 10^{-7}$ dynes, in the PBG nematic systems.

free energy rather than chain end entropy, which predicts

$$K_1 \approx EL^2 \approx \frac{kT}{d}\left(\frac{E}{ckT}\right)\phi\left(\frac{L}{d}\right), \tag{7}$$

where E^{-1} is the osmotic compressibility and c is the number density of chain ends. For fully extended chains, the leading behaviour of E is linear in c, and thus there is no disagreement between the qualitative description of Meyer's and de Gennes's models in the case of solutions.

The measured elastic moduli of PBG nematic liquid crystals are compared with the theoretical predictions summarized above in table 4. As is shown in table 4, the obvious interpretation of our results is that the short PBG molecules act as rigid rods, while above a certain length, as the molecules become more strongly coupled to the mean nematic ordering, their intrinsic flexibility makes them bend, so that the modulus saturates, while the splay modulus keeps increasing linearly with L/d.

Combining the arguments of the behavior of K_1 and K_3, we expect that around the crossover region, $K_1 \approx K_3$, which is in agreement with the data. The persistence length of PBG gives $P/d \approx 50$–80, in good agreement with our data, since the

Table 4. Comparison of the elastic moduli of the PBG nematic systems with existing theoretical predictions as a function of L/d ($\phi \approx 0{\cdot}16$)

Ratio	PBG L/d = 30–50	Rigid rods	PBG L/d = 50–100	Semiflexible chains
K_3/K_1	$(L/d)^{\alpha}$ $(1 \leqslant \alpha \leqslant 2)$	$[\phi(L/d)]^{\beta}$ $(1 \leqslant \beta \leqslant 2)$	$1/(L/d)$	P/L
K_1/K_2	(L/d)	3	(L/d)	$\phi^{2/3}(L/d)(P/d)^{-1/3}$
K_3/K_2	$(L/d)^{1+\alpha}$	$[\phi(L/d)]^{\beta}$	Constant	$\phi^{2/3}(P/d)^{2/3}$

crossover should begin for L/d somewhat less than P/d. The previous studies of the concentration dependence of the elastic moduli [24] were performed for samples near the crossover length, and are consistent with the interpretation given here.

4.2. *Viscosity coefficients*

We now examine the behaviour of effective viscosity coefficients as a function of L/d. For low-molecular-weight nematics, understanding the relative values of viscosities

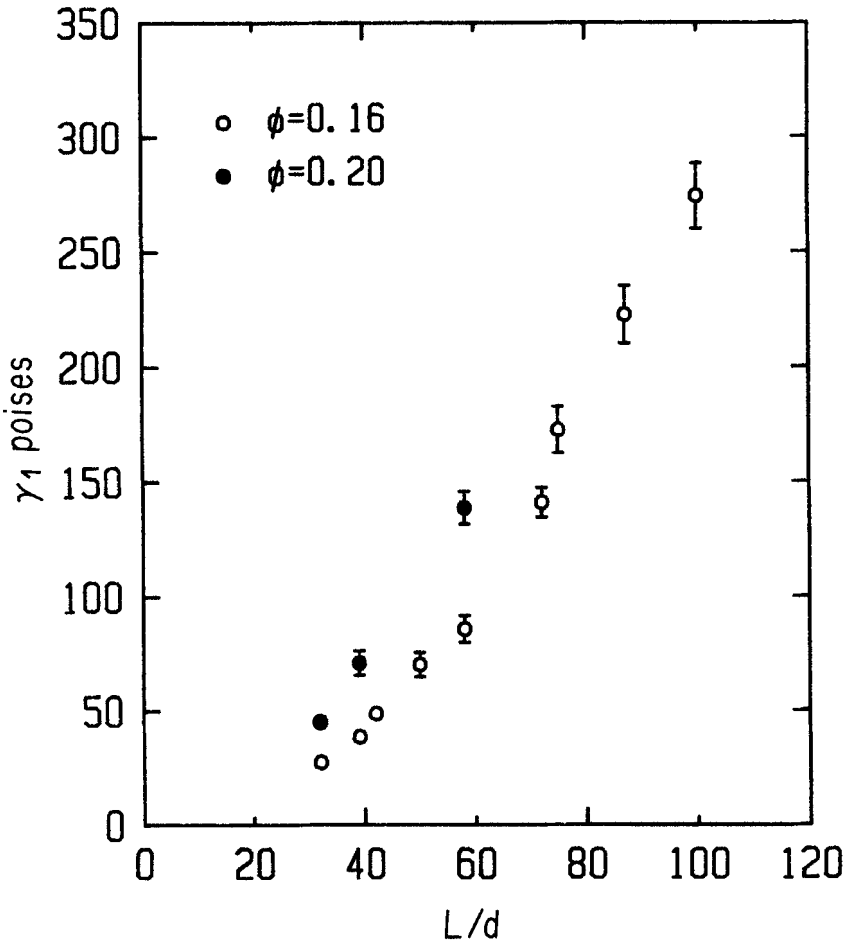

Figure 7. Twist viscosity, γ_1, as a function of L/d, assuming $K_2 = 0{\cdot}6 \times 10^{-7}$ dynes, in the PBG nematic systems.

is difficult, but for very long chains, some simplifications are expected, [16] which we see in our data. The viscosity associated with splay, η_{splay}, is found to approach that for twist, γ_1, with increasing L/d. The splay distortion involves cooperative director rotations coupled to limited sliding of the polymers parallel to one another, the two processes facilitating each other. In the limit of very long chain length, the viscosity for pure rotation of the director, γ_1, becomes extremely large compared to η_b, the shear viscosity for sliding of the polymers along one another, so that it dominates the behaviour of the splay viscosity, as we observe. Moreover, one of the other simple shear viscosities, η_c, should approach γ_1 in the long chain limit. The ratio η_c/η_b, identical to the ratio η_{splay}/η_{bend} which we measured, is found to be on the order of 10^2, which supports our conclusions about the splay viscosity. The bend distortion is the only one that has a low viscosity, which approaches η_b, as L increases, another characteristic of the very long chain limit.

Again assuming K_2 constant, we extract absolute values for viscosities from our data. The chain length dependences of the viscosities γ_1 and η_{bend} were illustrated in figures 7 and 8, respectively. The anisotropy between γ_1 and η_{bend} is huge and increasing

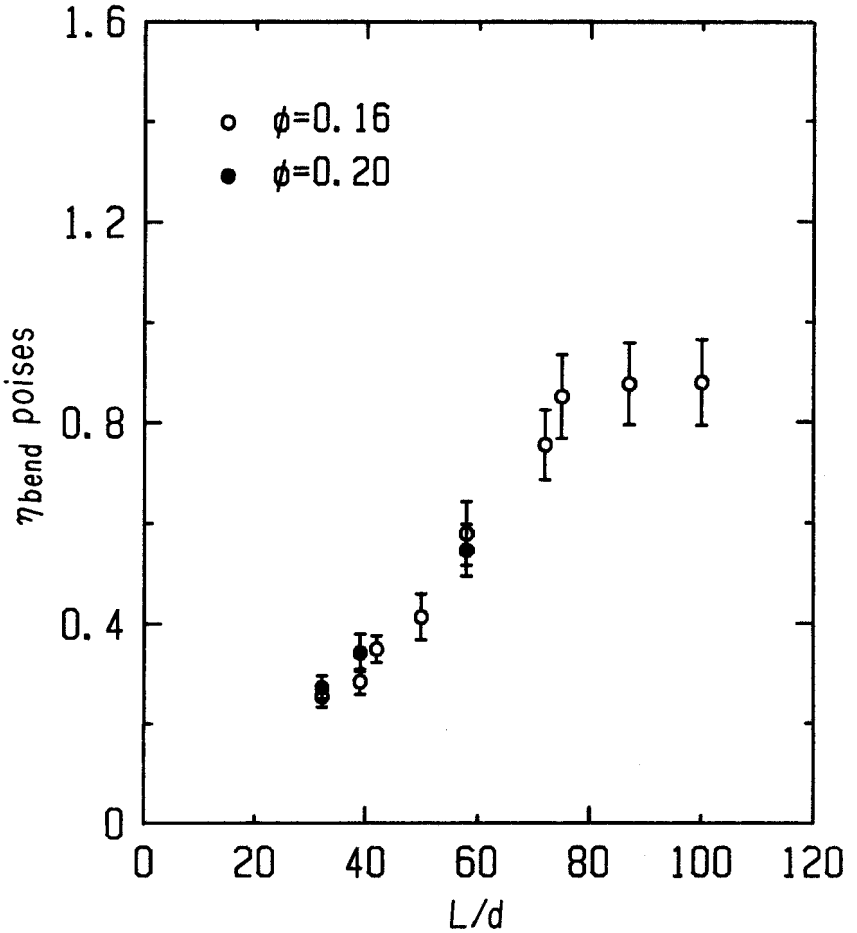

Figure 8. Bend viscosity, η_{bend}, as a function of L/d, assuming $K_2 = 0{\cdot}6 \times 10^{-7}$ dynes, in the PBG nematic systems.

with L/d. An approximately quadratic dependence for γ_1, and two distinctly different dependencies for η_{bend} are observed. The main features are generally in accord with the following qualitative ideas. For highly parallel molecules, in the rigid rod regime, η_c and γ_1 are large, and both should grow as $(L/d)^2$, by a simple geometrical argument [16]. Also in this regime, η_b is small, but increases with increasing L/d due to inter-particle interference effects. As the polymer becomes longer and therefore semi-flexible, but fully extended, η_c and γ_1 grow with L/d in a way that is essentially unchanged from the rigid rod limit as long as chain entanglements are not very strong. However, for η_b, once the polymers bend with the director field, inter-particle interference effects no longer grow with chain length, and η_{bend} becomes identical to η_b. In the absence of entanglement effects, η_b eventually saturates becoming independent of L/d. This should occur for $L \approx P$, which is what we observe. The results for ratios of several viscosities are also compared with molecular kinetics description [29–31] together with the infinite chain limit [16], in table 5. It is noted that for $L/d = 50$ PBG already approaches a behavior characteristic of the infinite chain limit.

5. Concluding remarks

We have performed quasi-elastic Rayleigh scattering measurements on the well aligned nematic liquid crystals of poly-γ-benzyl glutamate (PBG) to determine their elastic moduli and nematodynamic viscosity coefficients as a function of molecular chain length. We have observed for the first time the crossover, as a function of chain length, from rigid to semiflexible behavior of the anisotropic viscoelastic coefficients for a PBG nematic liquid crystal. By the time the crossover begins, for $L/d \approx 50$, this system is also exhibiting behaviour characteristic of the infinite chain limit. As shown in table 4 and table 5, the experimental results are in reasonably good agreement with current theoretical predictions, even though quantitative comparison is still hard to achieve. We see that for both elasticity and viscosity, the bend distortions of an individual polymer, coupled to the director distortions, play a significant role in determining the mechanical properties of this system.

Table 5. Comparison of ratios of several viscosities in the PBG nematic systems with molecular kinetic descriptions. $q \approx \phi(L/d)$ and $0 < \lambda < 1$ is a parameter.

Ratio	PBG	Infinite chain limit ([16]: $L \to \infty$)	Molecular kinetic theory ([31]: $q \to \infty$)
η_{splay}/γ_1	0·85–1·00	1	$1 - 1\pi/2\lambda q^{-2}$
η_{bend}/γ_1	$<0{\cdot}01$	0	$\lambda\pi/8q^{-2}$
η_b/η_c	$\leqslant 0{\cdot}01$	0	$\lambda\pi/8q^{-2}$
γ_1/η_c	≈ 1	1	$1 + (4 - \lambda)\pi/8q^{-2}$

Finally, the temperature may be an interesting parameter for the complete description of the macroscopic properties of polymer liquid crystals. Most liquid-crystalline polymer systems are not perfectly athermal, but exhibit some degree of thermal behavior. The persistence length is directly affected by the variation in temperature, and thus the study of bending fluctuations of a polymer chain may provide valuable information on its flexibility mechanism in the nematic state.

We are very grateful to Professor E. T. Samulski for helpful suggestions on sample preparation. This research was supported in part by the National Science Foundation

through Grant No. DMR-8803582, and by the Martin Fisher School of Physics, Brandeis University.

References

[1] LONBERG, F., FRADEN, S., HURD, A. J., and MEYER, R. B., 1984, *Phys. Rev. Lett.*, **52**, 1903. LONBERG, F., and MEYER, R. B., 1985, *Phys. Rev. Lett.*, **55**, 718.
[2] MEYER, R. B., LONBERG, F., TARATUTA, V., FRADEN, S., LEE, S-D., and HURD, A. J., 1985, *Discuss. Faraday chem. Soc.*, **79**, 125.
[3] CIFERRI, A., and WARD, I. M., 1979, *Ultra-high Modulus Polymers* (Applied Science Publisher).
[4] DEGENNES, P. G., 1974, *The Physics of Liquid Crystals* (Clarendon Press).
[5] LEE, S.-D., and MEYER, R. B., 1988, *Phys. Rev. Lett.*, **61**, 2217.
[6] DUPRE, D. B., and DUKE, R. W., 1975, *J. chem. Phys.*, **63**, 143.
[7] SRIDAR, C. G., HINES, W. A., and SAMULSKI, E. T., 1974, *J. chem. Phys.*, **61**, 947.
[8] MURTHY, N. S., KNOX, J. R., and SAMULSKI, E. T., 1976, *J. chem. Phys.*, **65**, 4835.
[9] TARATUTA, V., HURD, A. J., and MEYER, R. B., 1985, *Phys. Rev. Lett.*, **55**, 246.
[10] BLOCK, H., 1983, *Poly(γ-benzyl-L-glutamate) and Other Glutamic Acid Containing Polymers* (Gorden & Breach).
[11] NAKAMURA, H., HUSIMI, Y., JONES, G. P., and WADA, A., 1977, *J. chem. Soc. Faraday Trans. II*, **73**, 1178.
[12] VITOVSKAYA, M. G., and TSVETKOV, V. N., 1976, *Eur. Polym. J.*, **12**, 251.
[13] PAULING, L., and COREY, R. B., 1951, *Proc. natn. Acad. Sci.*, **37**, 235.
[14] SAMULSKI, E. T. (private communication).
[15] MITCHELL, J. C., WOODWARD, A. E., and DOTY, P., 1957, *J. Am. chem. Soc.*, **79**, 3955.
[16] MEYER, R. B., 1982, *Polymer Liquid Crystals*, edited by A. Ciferri, W. R. Krigbaum and R. B. Meyer (Academic Press), Chap. 6.
[17] UEMATSU, Y., TOMIZAWA, J., KIDOKORA, F., and SASAKI, T., 1979, *Polym. J.*, **2**, 53.
[18] DUPRE, D. B., 1982, *Polymer Liquid Crystals*, edited by A. Giferre, W. R. Krigbaum and R. B. Meyer (Academic Press), Chap. 6.
[19] TARATUTA, V., SRAJER, G., and MEYER, R. B., 1985, *Molec. Crystals liq. Crystals*, **116**, 245.
[20] ORSAY GROUP ON LIQUID CRYSTALS, 1969, *J. chem. Phys.*, **51**, 816.
[21] ORSAY GROUP ON LIQUID CRYSTALS, 1969, *Phys. Rev. Lett.*, **51**, 816.
[22] For a comprehensive discussion, see DE GENNES, P. G., 1974, *The Physics of Liquid Crystals* (Clarendon Press), Chap. 5.
[23] TORIUMI, H., MATSUZAWA, K., and UEMATSU, I., 1984, *J. chem. Phys.*, **81**, 6085.
[24] TARATUTA, V. G., LONBERG, F., and MEYER, R. B., 1988, *Phys. Rev.* A, **37**, 1831.
[25] STRALEY, J. P., 1973, *Phys. Rev.* A, **8**, 2181. PONIEWIERSKI, A., and STECKI, J., 1979, *Molec. Phys.*, **39**, 1931.
[26] LEE, S.-D., and MEYER, R. B., 1986, *J. chem. Phys.*, **84**, 3443.
[27] ODIJK, T., 1986, *Liq. Crystals*, **1**, 553.
[28] DEGENNES, P. G., 1977, *Molec. Crystals liq. Crystals Lett.*, **34**, 177.
[29] MARRUCCI, G., 1982, *Molec. Crystals liq. Crystals*, **72**, 153.
[30] KUZUU, N., and DOI, M., 1983, *J. phys. Soc. Japan*, **52**, 3486; 1984, *Ibid.*, **53**, 1031.
[31] LEE, S.-D., 1988, *J. chem. Phys.*, **88**, 5196.